Supporting Information

for

Remote Detection of HCN, HF, and Nerve Agent Vapors Based on Self-Referencing, Dye-Impregnated Porous Silicon Photonic Crystals

Yi-Sheng Lu[†], Sanahan Vijayakumar[†], Arnaud Chaix[‡], Brian R. Pimentel[‡], Kyle C. Bentz[‡], Sheng Li[∥], Adriano Chan[∥], Charlotte Wahl[§], James S. Ha[§], Deborah E. Hunka[§], Gerry R. Boss[∥], Seth M. Cohen[†‡], Michael J. Sailor[†‡*]

[†]Materials Science and Engineering Program, University of California, San Diego, La Jolla, California 92093, United States

[‡]Department of Chemistry and Biochemistry, University of California, San Diego, La Jolla, California 92093, United States

[§]Leidos, 10260 Campus Point Drive, San Diego, CA 92121

[∥]Department of Medicine, University of California, San Diego, La Jolla, California 92093, United States
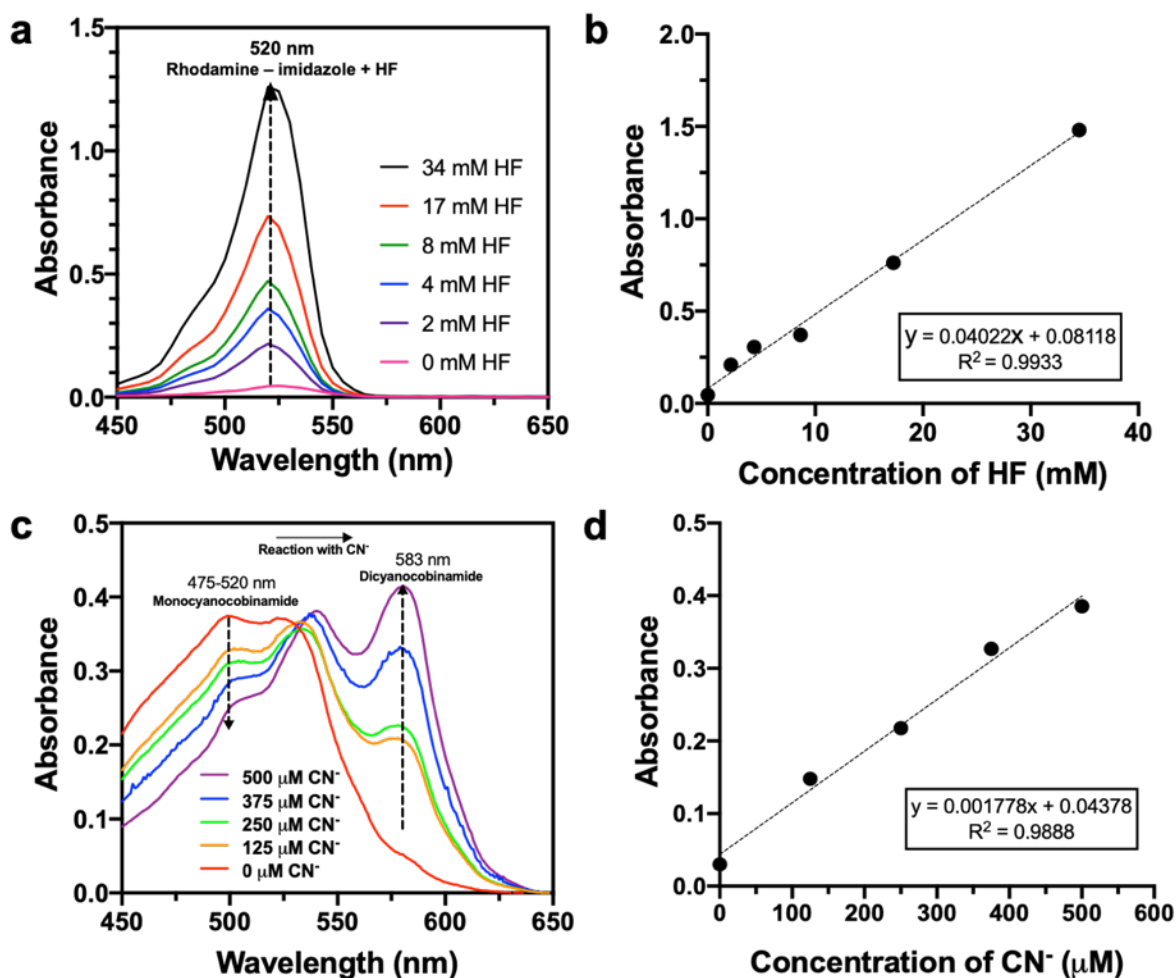
*Corresponding author

Figure S1. (a) Series of UV-vis absorbance spectra of rhodamine – imidazole (RDI) indicator dye (2 mM) in 1:1 (v:v) acetonitrile:dichloromethane solution, upon titration with HF to the indicated values. (b) Dose-response curve extracted from (a), showing RDI absorbance at 520 nm as a function of HF concentration, over the range 0 – 34 mM. The measured molar extinction coefficient of RDI at 520 nm for the condition of [HF] = 34 mM is 40.22 M^{-1} cm^{-1}. (c) Series of UV-vis absorbance spectra of monocyanocobinamide (MCbi) indicator dye (500 μM) in water, upon titration with CN^- to the indicated values. (d) Dose-response curve extracted from (c), showing MCbi absorbance at 583 nm as a function of different concentrations of CN^- (0 – 500 μM). The measured molar extinction coefficient of MCbi at 520 nm for the condition of [CN^-] = 500 μM is 1778 M^{-1} cm^{-1}.
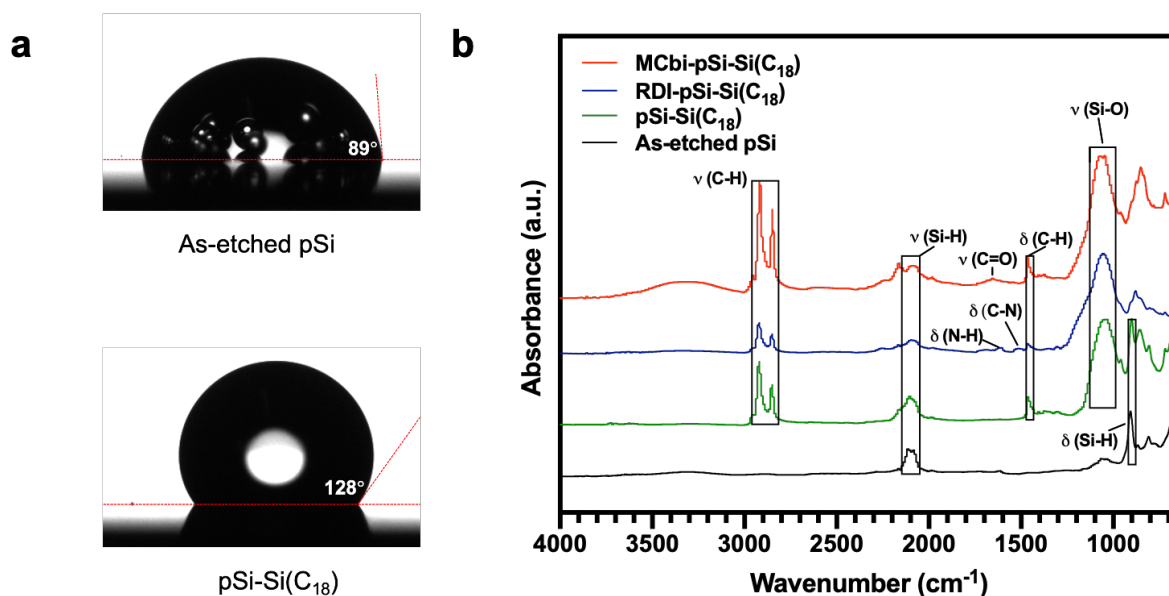
Figure S2. Characterization of surface chemistry of RDI-pSi and MCbi-pSi photonic crystal sensors. (a) Images showing water contact angle on as-etched pSi and the chemically modified pSi-Si(C_{18}), prepared by thermal dehydrocoupling of octadecylsilane to pSi. Contact angle values reported are averages from 3 separate samples. Bubbles apparent in the image of the as-etched pSi sample are attributed to hydrogen, resulting from chemical reaction of pSi with water. (b) Attenuated total reflectance Fourier-transform infrared (ATR-FTIR) spectra of modified sensor samples, from bottom to top: As-etched pSi (black trace), pSi-Si(C_{18}) (green trace). RDI-pSi-Si(C_{18}) (blue trace) and Cbi-pSi-Si(C_{18}) (red trace). Symbols: ν = stretching, δ = bending.
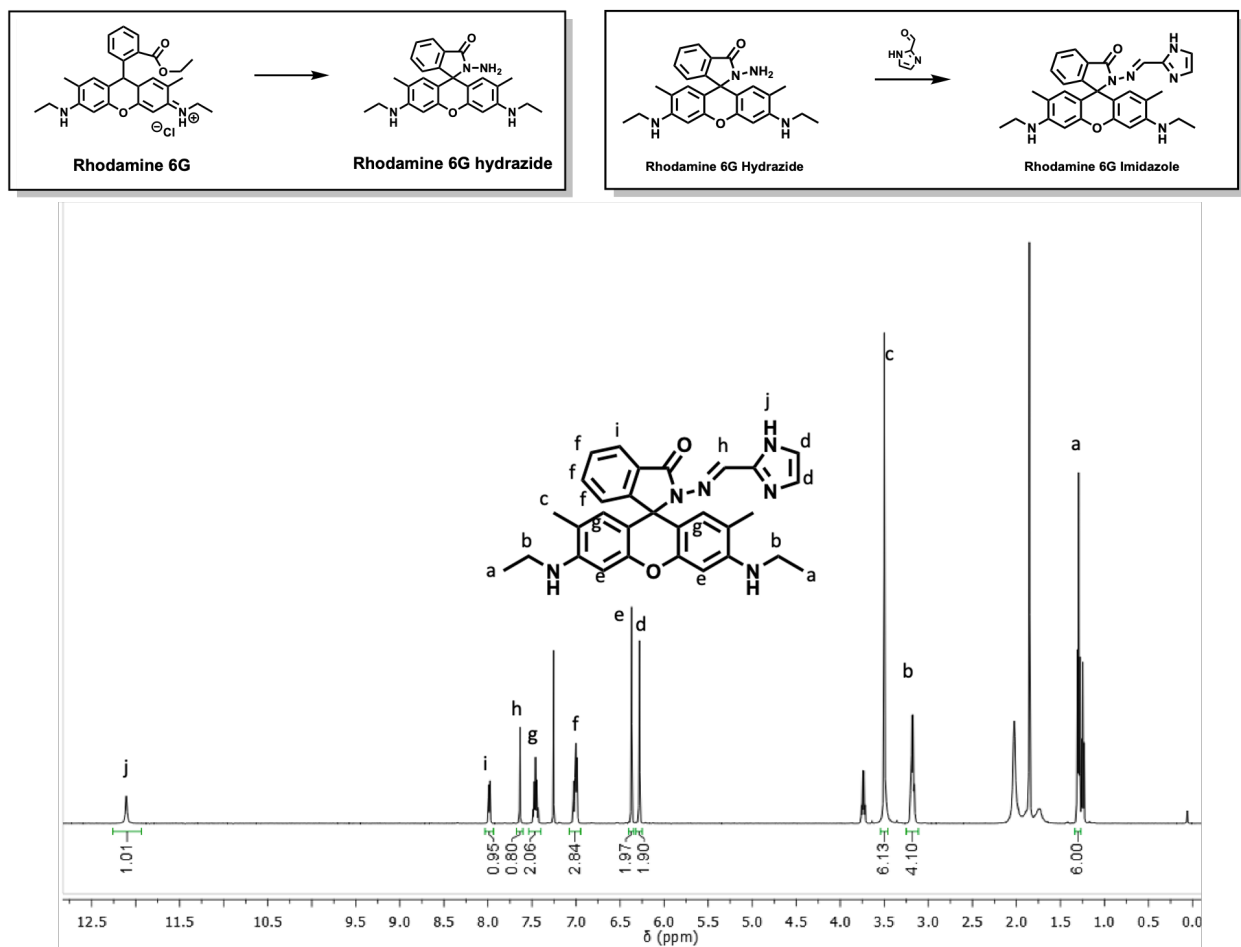
Figure S3. Reaction scheme used for preparation of the rhodamine 6G-imidazole complex referred to in this work as as "RDI" or "Rhodamine-imidazole" (above), and the ^{1}H NMR spectrum of the RDI product in CDCl$_3$ (below). Peak at 0 ppm is TMS reference. The synthesis of RDI followed the procedure described in the literature.[1, 2]
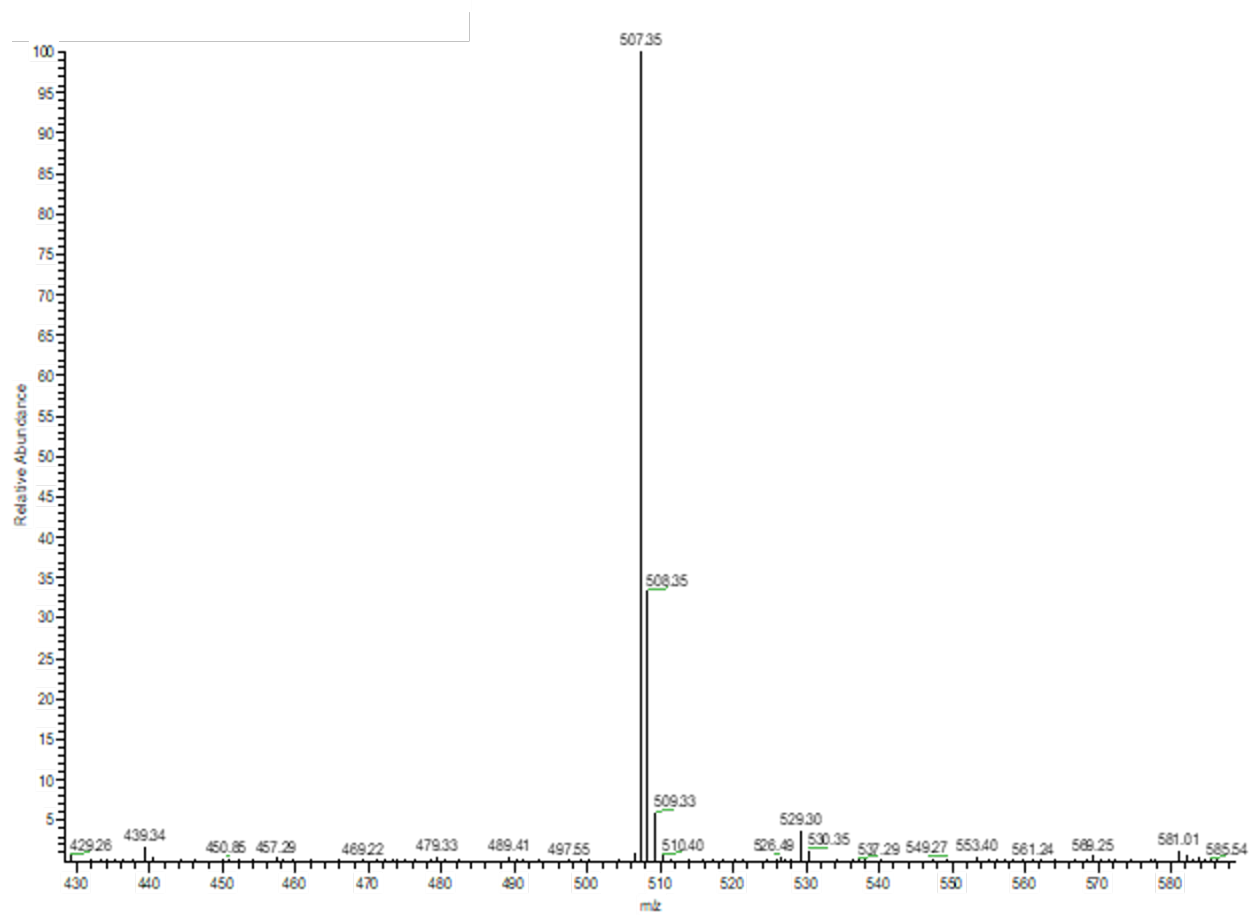
Figure S4. ESI-MS spectrum of RDI. Ion at m/z = 507.35 is assigned to [RDI+H]$^{+}$ parent ion.
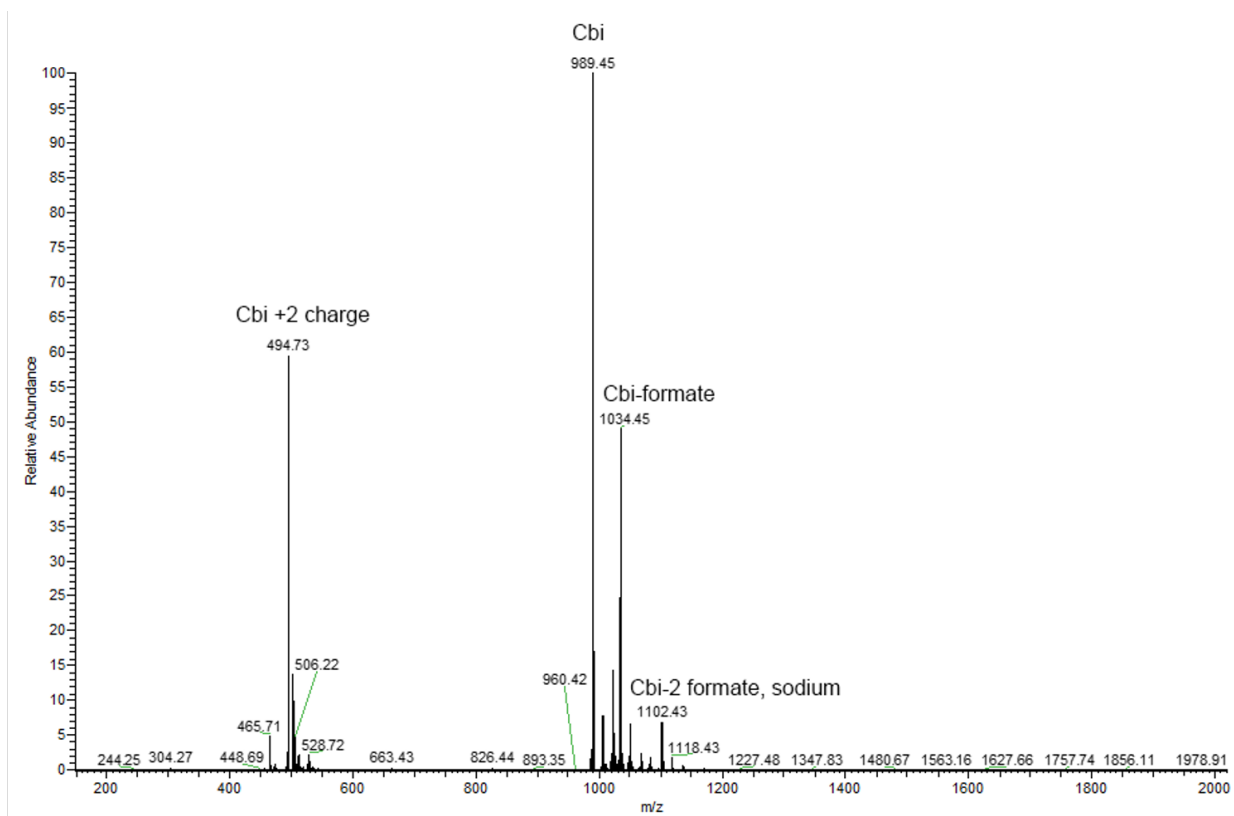
Figure S5. ESI-MS spectrum of cobinamide, referred to in this work as "Cbi." Parent ion, dipositive parent, and formate adducts assigned. Sodium formate was added to the sample prior to measurement to improve detection.
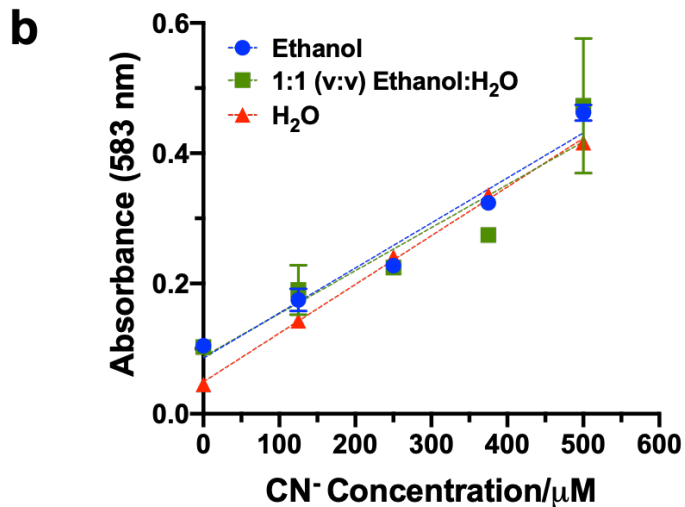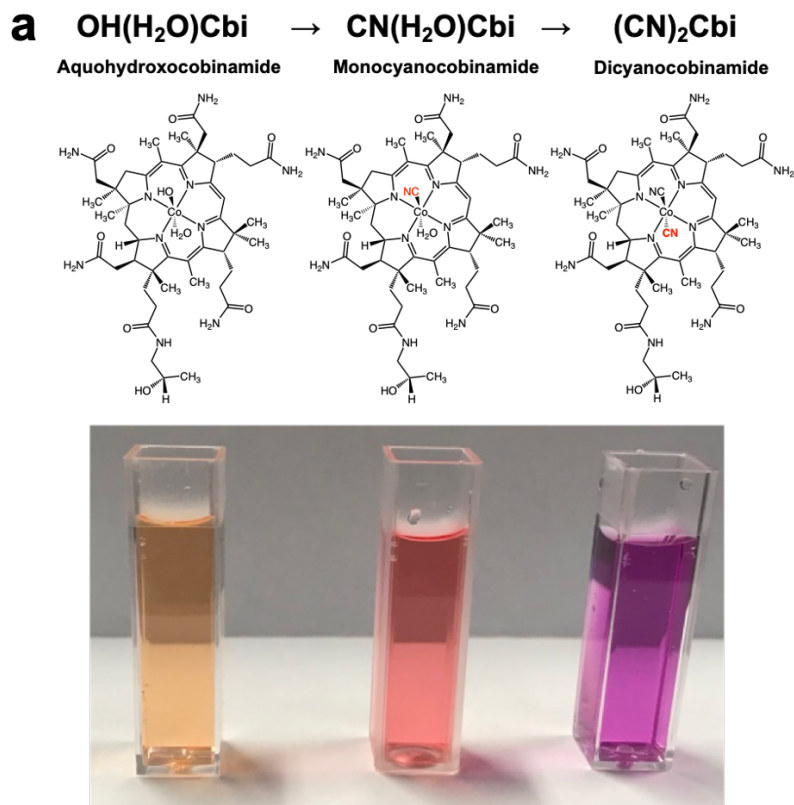
Figure S6. (a) Molecular structures of aquohydroxocobinamide, monocyanocobinamide and dicyanocobinamide. Photograph of corresponding cuvettes containing solutions of the three species is shown at the bottom. Monocyanocobinamide ("CN(H₂O)Cbi", or "MCbi") used in this work was prepared in-situ by reaction of an equimolar mixture of aquohydroxocobinamide and KCN. (b) Calibration curve showing MCbi absorbance at a wavelength of 583nm as a function of CN⁻ concentration (in micromolar; 0 – 500 μM) in water, 1:1 (v:v) ethanol:water mixture and ethanol. Data shown no significant solvatochromism. The error bars shown are the standard deviation of triplicate trials.
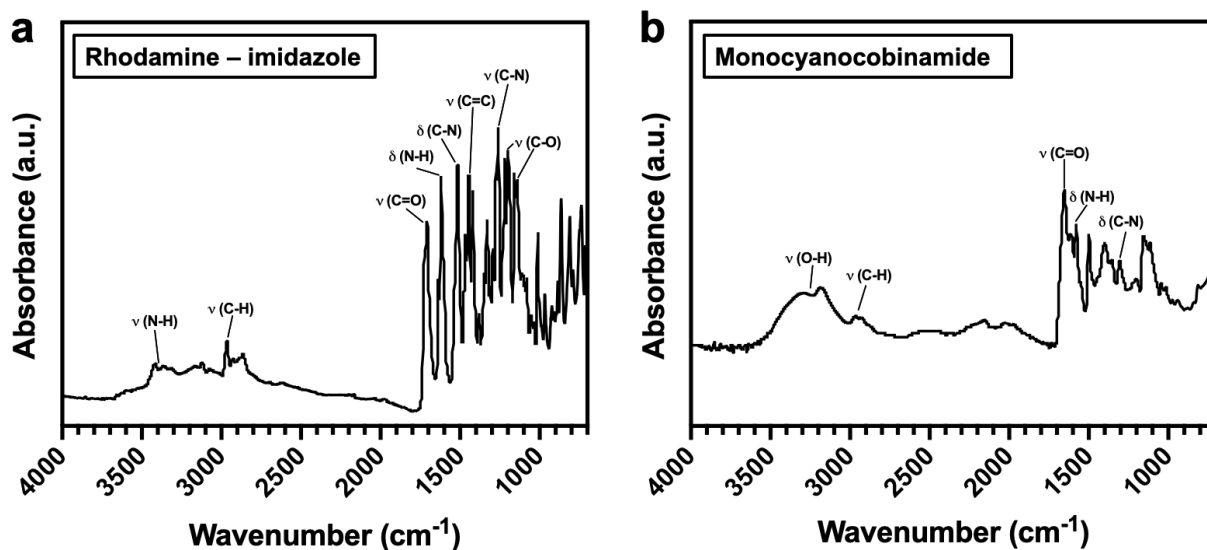
Figure S7. Attenuated total reflectance Fourier-transform infrared (ATR-FTIR) spectra of (a) Rhodamine – imidazole (RDI) and (b) Monocyanocobinamide (MCbi). Spectra obtained from dry powder samples.
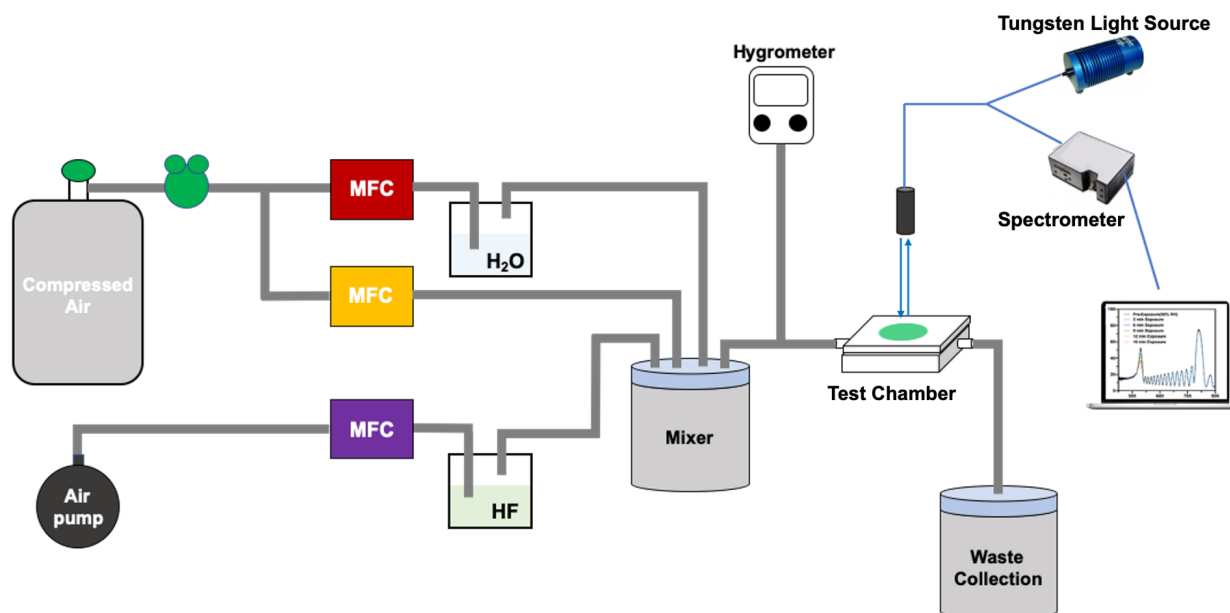
Figure S8. Schematic of vapor dosing setup for HF, HCl, NH_3, and octane vapor sensing experiments (example for HF analyte is shown; the setup for the other analytes was similar). Mass Flow Controllers (MFC) enabled control of the overall analyte concentration, flow rate and % RH (which was measured with a commercial hygrometer). Mass flow rates of pure air, humid air (air bubbled through "H_2O" reservoir) and analyte (air bubbled through "HF" reservoir) were adjusted to obtain the desired values of humidity and analyte concentration in the "Mixer" chamber. The total flow rate of carrier gas for sensor dosing was 300 sccm. The volume of the mixer and testing chamber was approx. 500.0 cc; the concentration of analyte in the testing chamber was assumed to reach the steady-state, set-point concentration after 5 volumes had passed through the chamber, corresponding to 5 x 500.0/300sccm = 8.3 min.

For $HF_{(g)}$ $HCl_{(g)}$, and $NH_{3(g)}$ analytes, concentration in the flow stream was set by placing an aqueous solution of the analyte (at a fixed concentration; see below) in the analyte reservoir and then bubbling the carrier gas through the solution. The aqueous concentration that would provide the desired analyte concentration in the gas phase was chosen based on published vapor pressure values of $HF_{(g)}$ and $HCl_{(g)}$[3, 4] and calculated vapor pressure of $NH_{3(g)}$ using temperature-dependent Henry's Law constant[5] and assuming the air in the stream obtained the published value of the equilibrium vapor pressure of analyte upon passing through the solution (temperature of the solution was 25 ± 2 °C). The following values were used:

Concentration of HF solution (M)	Partial Pressure of HF Vapor (mmHg)
1.725	0.0598
0.575	0.0284
0.0575	0.0157

Concentration of HCl solution (M)	Partial Pressure of HCl Vapor (mmHg)
6	0.0903
7	0.231

Concentration of NH_3 solution (M)	Partial Pressure of NH_3 Vapor (mmHg)
0.00690	0.0844
0.00931	0.114
0.0310	0.380

The octane analyte was treated similarly, except that neat octane was used, and so the partial pressure of analyte in the carrier gas was assumed to be 11.8 mmHg[6] (the published vapor pressure of octane at 25 °C).
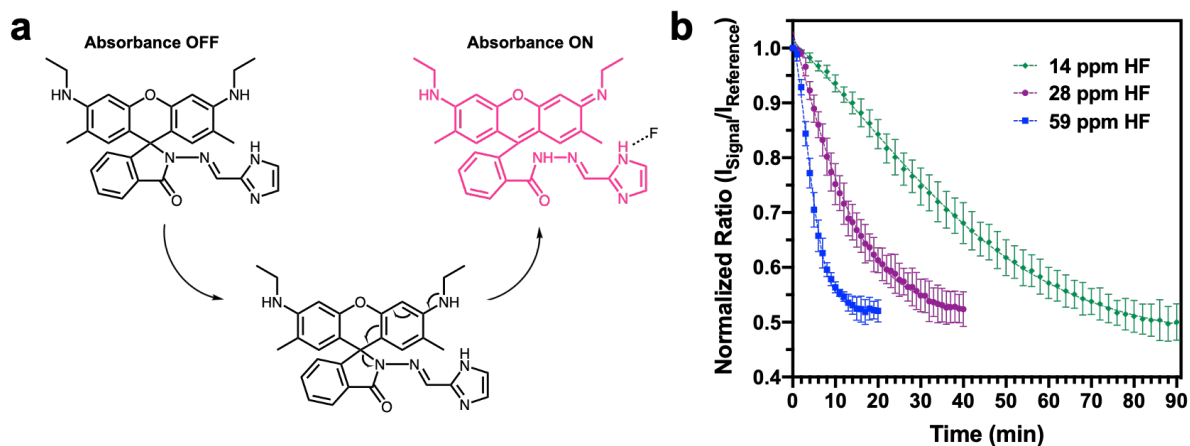
Figure S9. (a) Reported mechanism of HF detection by Rhodamine (RDI)[2] and (b) Temporal response curves of RDI – pSi photonic crystal sensor with 14 – 59 ppm HF vapor under 50% RH. The data were acquired every two minutes and the error bars shown represent the standard deviation of triplicate trials.
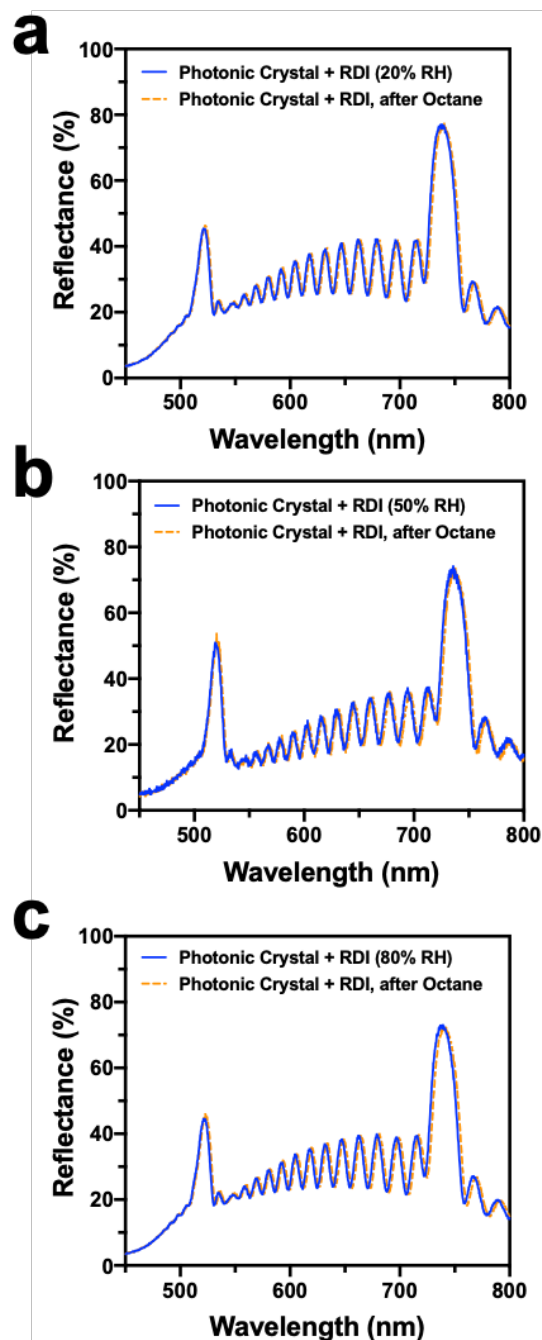
Figure S10. Optical reflectance spectra of RDI-photonic crystal sensor, recorded before and after exposure to 600 ppm octane at (a) 20% RH, (b) 50% RH and (c) 80% RH for 10 min. The stop bands all display a slight (< 3 nm) red shift upon introduction of octane vapor, attributed to adsorption of this vapor in the mesoporous structure. Upon exposure to octane, the intensity of the band at 520 nm displayed a small but consistent increase in intensity, whereas the intensity of the band at 740 nm displayed a small but consistent decrease in intensity. This derives from the instrumental spectral response function, which was not corrected for in these data.
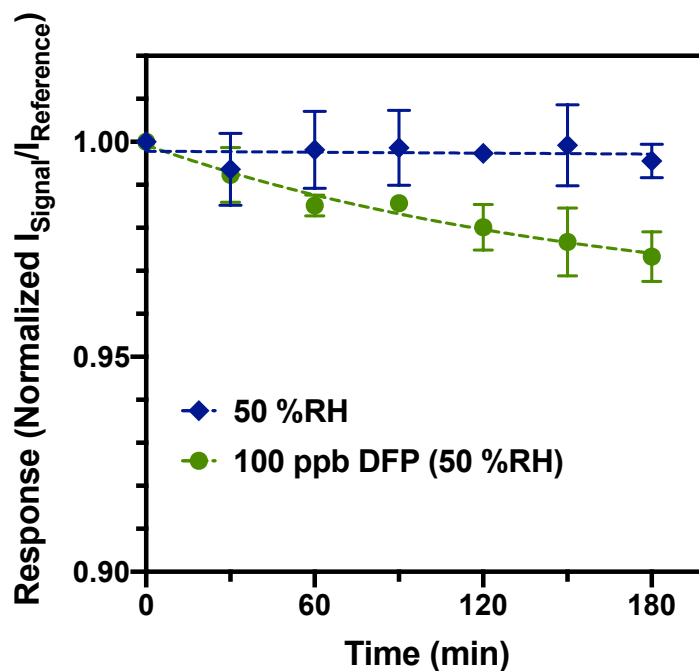
Figure S11: Temporal response curve of RDI – pSi photonic crystal sensors to 100 ppb of DFP vapor under 50% RH. DFP vapor (228 ppb) was generated in a permeation tube oven at 50°C and diluted 1:1 v:v into humidified (100% RH) laboratory air, resulting in a final concentration of 114 ppb of DFP and 50% RH. The data were acquired every 30 minutes. The error bars shown are standard deviation of triplicate trials.
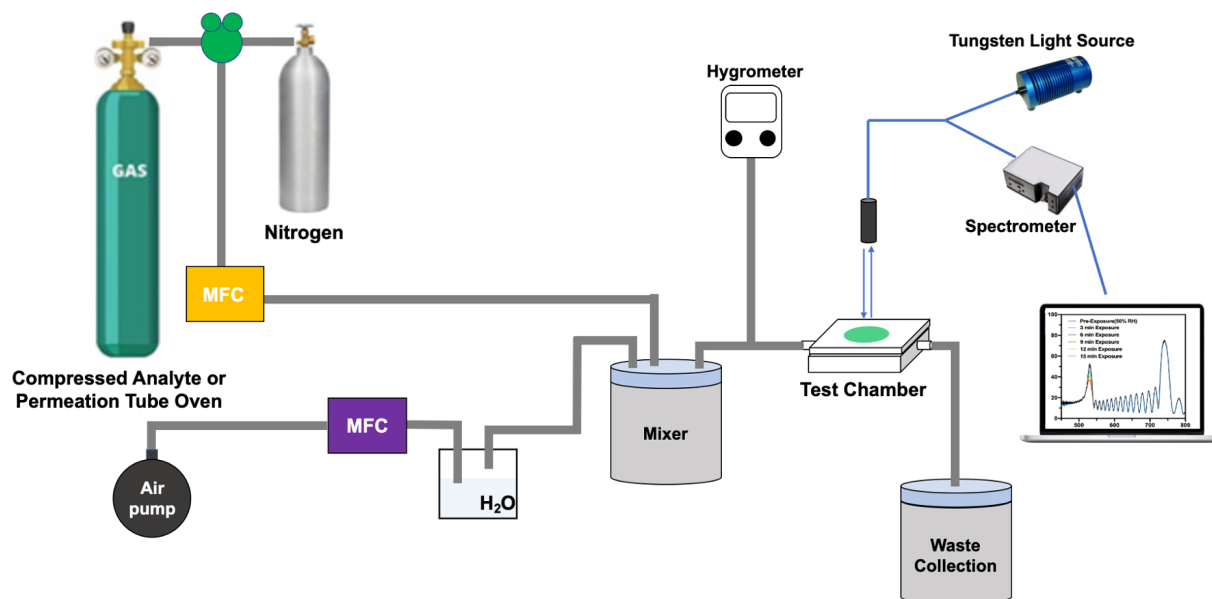
Figure S12: Schematic of vapor dosing setup for HCN and DFP sensing. The source of HCN was a certified gas cylinder ("compressed analyte") containing either 10 or 20 ppm HCN in dry nitrogen. The source of DFP was a VICI Metronics Dynacalibrator Model 190 vapor generator that used certified permeation tubes from KIN-TEK Analytical, Inc. that contained DFP. The device was programmed to deliver 228 ppb of DFP vapor at 50 °C into dry nitrogen carrier gas. The RH values reported were monitored with a probe hygrometer. The HCN sensing experiments were conducted with a flow rate of 300 sccm, and the DFP sensing experiments were conducted with a flow rate of 100 sccm. The Mass Flow Controllers (MFC) enabled control of the overall analyte concentration, flow rate and % RH (which was measured with a commercial hygrometer). Mass flow rates of humid air (air bubbled through "H_2O" reservoir) and analyte (diluted with from calibrated gas cylinder or vapor generator as shown) were adjusted to obtain the desired values of humidity and analyte concentration in the "Mixer" chamber. The volume of the mixer and testing chamber was approx. 500.0 cc; the concentration of analyte in the testing chamber was assumed to reach the steady-state, set-point concentration after 5 volumes had passed through the chamber, corresponding to 5 x 500.0/300sccm = 8.3 min.
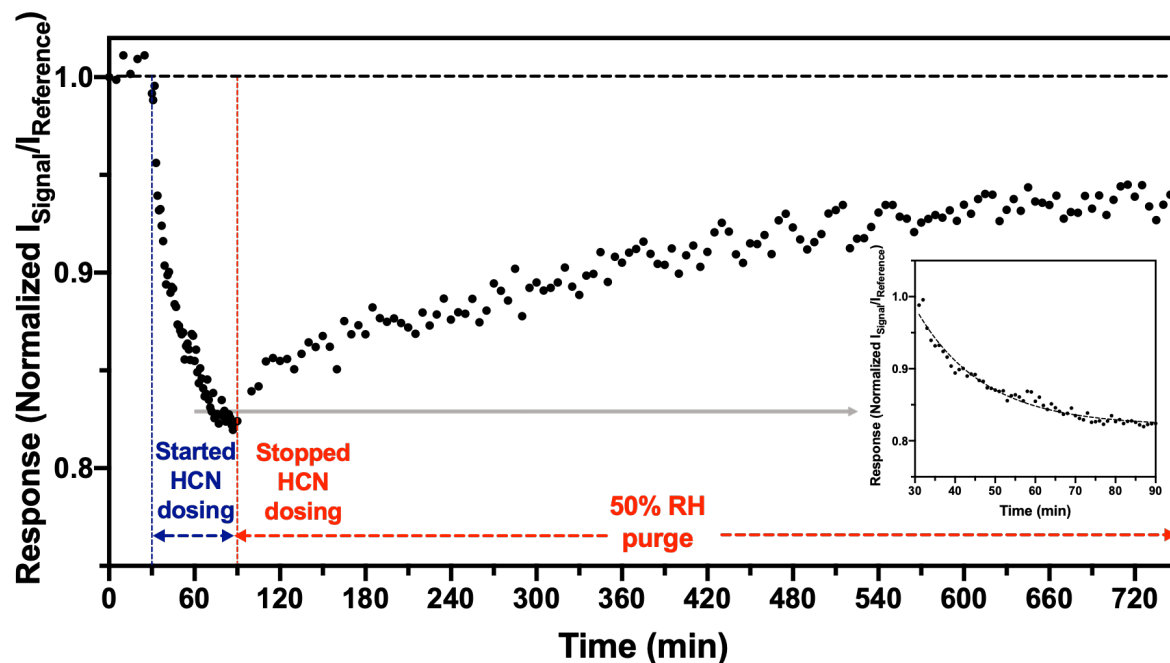
Figure S13: Representative temporal response curve of a MCbi – pSi photonic crystal sensor to sequential exposure of 50% RH air (time = 0 to 30 min); 10 ppm of HCN vapor in 50% RH air; (time = 30 to 90 min); 50% RH purge (time = 90 to 750 min). The optical responses were acquired every min for the dosing of HCN vapor, and every 5 min for the conditions of 50% RH of air and 50% RH purge. The inset shows an expansion of the portion of the sensor response curve during exposure to 10 ppm HCN vapor in 50% RH (from time = 30 to 90 min).
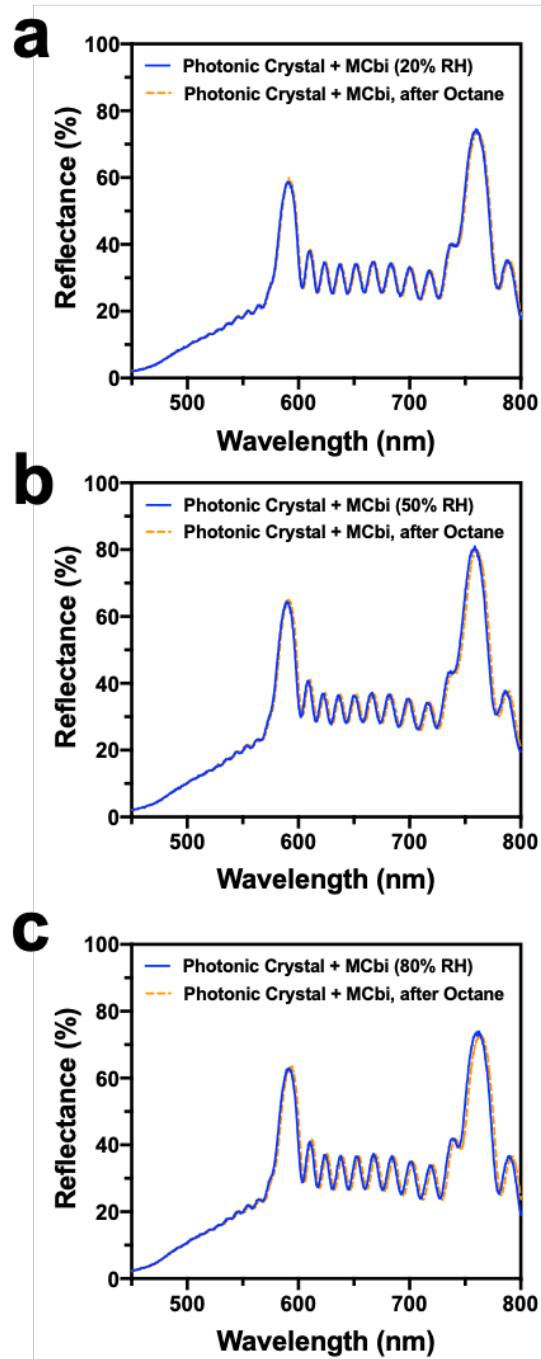
Figure S14. Optical reflectance spectra of MCbi-photonic crystal sensor before and after exposure to 600 ppm octane at (a) 20% RH, (b) 50% RH and (c) 80% RH for 10 min. The stop bands all display a slight (< 3 nm) red shift upon introduction of octane vapor, attributed to adsorption of this vapor in the mesoporous structure.
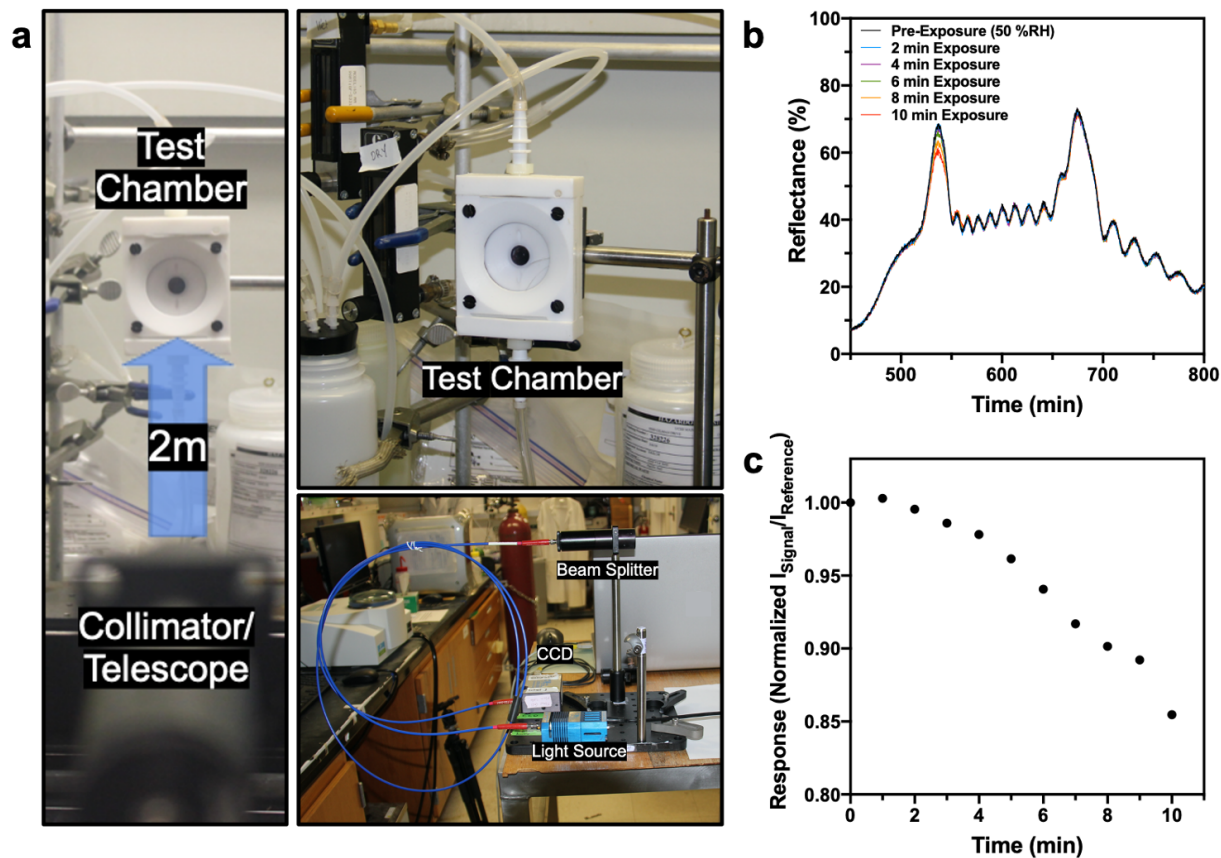
Figure S15: Experimental setup and representative data for remote sensing of HF vapor. (a) Photographs of the remote sensing configuration. Fiber optic cables from a tungsten lamp (Light Source) and from a charge coupled device (CCD) spectrometer were combined into a dual bifurcated fiber, and the distal end was fed into collimator optics (Collimator/Telescope) positioned 2 meters from the pSi photonic crystal sensor, which was mounted in a test chamber fitted with an optical window. (b) Overlaid reflectance spectra, obtained at the indicated time points, for a RDI-pSi photonic crystal sensor exposed to 28 ppm of HF vapor at 0, 2, 4, 6, 8 and 10 minutes at 50% RH. (c) Temporal response (see eq. 2 in the text) of RDI – pSi photonic crystal sensor upon exposure to 28 ppm HF vapor in air at 50% RH.

Literature Cited

1. Zhang, Z.; Zheng, Y.; Hang, W.; Yan, X.; Zhao, Y. Sensitive and selective off–on rhodamine hydrazide fluorescent chemosensor for hypochlorous acid detection and bioimaging. *Talanta* **2011,** *85*, 779-786.
2. Sivaraman, G.; Chellappa, D. Rhodamine based sensor for naked-eye detection and live cell imaging of fluoride ions. *J. Mater. Chem. B* **2013,** *1*, 5768-5772.
3. Brosheer, J.; Lenfesty, F.; Elmore, K. Vapor Pressure of Hydrofluoric Acid Solutions. *Ind. Eng. Chem.* **1947,** *39*, 423-427.
4. Fritz, J. J.; Fuget, C. R. Vapor Pressure of Aqueous Hydrogen Chloride Solutions, 0° to 50° C. *Ind. Eng. Chem. Chem. Eng. Data Series* **1956,** *1*, 10-12.
5. Clegg, S. L.; Brimblecombe, P. Solubility of ammonia in pure aqueous and multicomponent solutions. *J. Phys. Chem.* **1989,** *93*, 7237-7248.
6. Carruth, G. F.; Kobayashi, R. Vapor pressure of normal paraffins ethane through n-decane from their triple points to about 10 mm mercury. *J. Chem. Eng. Data* **1973,** *18*, 115-126.